AJNR

MR Imaging Characteristics Associate with Tumor-Associated Macrophages in Glioblastoma and Provide an Improved Signature for Survival Prognostication

J. Zhou, M.V. Reddy, B.K.J. Wilson, D.A. Blair, A. Taha, C.M. Frampton, R.A. Eiholzer, P.Y.C. Gan, F. Ziad, Z. Thotathil, S. Kirs, N.A. Hung, J.A. Royds and T.L. Slatter

AJNR Am J Neuroradiol 2018, 39 (2) 252-259
doi: https://doi.org/10.3174/ajnr.A5441
http://www.ajnr.org/content/39/2/252

MR Imaging Characteristics Associate with Tumor-Associated Macrophages in Glioblastoma and Provide an Improved Signature for Survival Prognostication

J. Zhou, M.V. Reddy, B.K.J. Wilson, D.A. Blair, A. Taha, C.M. Frampton, R.A. Eiholzer, P.Y.C. Gan, F. Ziad, Z. Thotathil, S. Kirs, N.A. Hung, J.A. Royds, and T.L. Slatter

ABSTRACT

BACKGROUND AND PURPOSE: In glioblastoma, tumor-associated macrophages have tumor-promoting properties. This study determined whether routine MR imaging features could predict molecular subtypes of glioblastoma that differ in the content of tumor-associated macrophages.

MATERIALS AND METHODS: Seven internally derived MR imaging features were assessed in 180 patients, and 25 features from the Visually AcceSAble Rembrandt Images feature set were assessed in 164 patients. Glioblastomas were divided into subtypes based on the telomere maintenance mechanism: alternative lengthening of telomeres positive (ALT+) and negative (ALT−) and the content of tumor-associated macrophages (with [M+] or without [M−] a high content of macrophages). The 3 most frequent subtypes (ALT+/M−, ALT−/M+, and ALT−/M−) were correlated with MR imaging features and clinical parameters. The fourth group (ALT+/M+) did not have enough cases for correlation with MR imaging features.

RESULTS: Tumors with a regular margin and those lacking a fungating margin, an expansive T1/FLAIR ratio, and reduced ependymal extension were more frequent in the subgroup of ALT+/M− ($P < .05$). Radiologic necrosis, lack of cystic component (by both criteria), and extensive peritumoral edema were more frequent in ALT−/M+ tumors ($P < .05$). Multivariate testing with a Cox regression analysis found the cystic imaging feature was additive to tumor subtype, and *O6-methylguanine methyltransferase* (*MGMT*) status to predict improved patient survival ($P < .05$).

CONCLUSIONS: Glioblastomas with tumor-associated macrophages are associated with routine MR imaging features consistent with these tumors being more aggressive. Inclusion of cystic change with molecular subtypes and *MGMT* status provided a better estimate of survival.

ABBREVIATIONS: ALT = alternative lengthening of telomeres; ALT− = alternative lengthening of telomeres negative; ALT+ = alternative lengthening of telomeres positive; *IDH* = *isocitrate dehydrogenase*; M+ = a tumor with a high content of tumor-associated macrophages; M− = a tumor with a low content of tumor-associated macrophages; *MGMT* = *O6-methylguanine methyltransferase*; PTE = peritumoral edema; VASARI = Visually AcceSAble Rembrandt Images

Glioblastomas are the most common and aggressive primary malignant brain tumor, with an incidence of 5.26 per 100,000 population.[1] With temozolomide and radiation therapy, the median survival is 14.6 months.[1] Patients' response to treatment and prognosis are notoriously variable. Many studies have attributed heterogeneous outcomes to molecular differences among glioblastomas, such as different means to maintain telomere integrity (telomerase activity or an alternative method known as the alternative lengthening of telomeres [ALT]).[2] In 2003, the presence of the ALT telomere maintenance mechanism was associated with longer patient survival compared with ALT negative (ALT−) tumors, including those that were telomerase positive (ALT+) and those where the telomere maintenance mechanism was unknown.[3]

It has been recently found that most tumors without a defined telomere maintenance mechanism contain a high con-

Received March 20, 2017; accepted after revision September 7.

From the Departments of Radiology (J.Z., M.V.R., B.K.J.W.) and Neurosurgery (A.T.), Southern District Health Board, Dunedin, New Zealand; Department of Pathology (J.Z., R.A.E., N.A.H., J.A.R., T.L.S.) and Surgical Sciences (A.T., S.K.), Dunedin School of Medicine, University of Otago, Dunedin, New Zealand; Departments of Radiology (D.A.B.), Neurosurgery (P.Y.C.G.), Pathology (F.Z.), and Medical Oncology (Z.T.), Waikato District Health Board, Hamilton, New Zealand; and Department of Medicine (C.M.F.), University of Otago, Christchurch, New Zealand.

This work was supported by the Health Research Council of New Zealand.

Paper previously presented at: American Roentgen Ray Society Annual Meeting, April 17–26, 2016; Los Angeles, California.

Please address correspondence to Dr. Jean Zhou, Department of Radiology, Dunedin Hospital, Southern District Health Board, 201 Great King St, Private Bag 1921, Dunedin, New Zealand; e-mail: jean.zhou@southerndhb.govt.nz

Indicates open access to non-subscribers at www.ajnr.org

Indicates article with supplemental on-line tables.

http://dx.doi.org/10.3174/ajnr.A5441

tent of tumor-associated macrophages (M+) that affects assays assigning telomere maintenance.[4] The revised subgroups were ALT positive tumors with and without (M−) a high content of macrophages (ALT+/M+ and ALT+/M−) and ALT negative tumors with and without a high content of macrophages (ALT−/M+ and ALT−/M−). With temozolomide treatment, patients with ALT−/M− tumors have improved survival compared with patients with ALT−/M+ tumors,[4] suggesting that identifying the increased macrophage content will distinguish those with a poor outcome.

MR imaging is a diagnostic tool that evaluates tumor as well as peritumoral characteristics. Improving prognostic determination based on MR imaging features alone has associated radiologic necrosis and peritumoral edema (PTE) with poorer survival.[5-8] Tumors with a cystic component have been associated with improved patient survival.[9,10] However, inconsistencies occur between studies, and MR imaging features are not always found as independent factors associated with survival.[11-14]

Imaging features have been attributed to differences in tumor biology, suggesting an analysis of MR imaging features combined with molecular characteristics may improve prognostic prediction. *Isocitrate dehydrogenase 1* (*IDH1*) mutations, *O6-methylguanine methyltransferase* (*MGMT*) promoter methylation, and epidermal growth factor receptor overexpressing tumors have been correlated with MR imaging features.[13,15-19] That tumor biology influences imaging features is further evident in studies that investigate subgroups of glioblastomas based on multiple gene expression differences.[20]

This study aimed to determine whether MR imaging features were associated with the telomere maintenance mechanism and tumor-associated macrophage content–based subtypes. The inclusion of MR imaging parameters with the molecular subtyping and *MGMT* promoter methylation status[21] was also investigated to determine whether it could better predict outcome for patients with glioblastoma.

MATERIALS AND METHODS

Study Participants

One hundred eighty patients from Dunedin, Christchurch, and Waikato hospitals in New Zealand with a diagnosis of glioblastoma between the years 2004 and 2014 were included in the study. The cohort was aged between 16–82 years (mean, 61 years; 95% CI, 59–63); 39% were female and 61% male; and 93% were white, 3% Maori, and 4% identified with other ethnic groups. All patients were eligible for standard of care therapy (surgery, radiation therapy, and temozolomide), and no patients received other therapies. The participants were all diagnosed with glioblastoma after the Stupp protocol was used in New Zealand.[1]

Participant Selection/Inclusion Criteria

The inclusion criteria were a diagnosis of glioblastoma (as assessed by 2 pathologists independently), no previous lower-grade brain tumor or other brain surgery, and no previous radiation or chemotherapy. No patients received corticosteroids at the time of the preoperative MR imaging scan. Survival time was defined as the time interval (months) between the time of diagnosis (defined as the time of the initial preoperative MR imaging scan) and death.

MR Imaging Features and Interpretation

Preoperative MR imaging scans were evaluated including T1, T2, FLAIR, and postcontrast T1-weighted sequences after intravenous infusion of 10 mL of gadolinium. Images were taken by clinical 1.5T (Siemens, Erlangen, Germany or GE Healthcare, Milwaukee, Wisconsin) scanners. All study scans had routine tumor protocol sequences (T1, T2, FLAIR, DWI, ADC, and postcontrast gadolinium T1), and some had additional susceptibility-weighted sequences. At least 3 reviewers (3 neuroradiologists [M.V.R., B.K.J.W., and D.A.B.] and 1 radiology registrar [J.Z.]) read each MR imaging scan independently in the Public Hospital PACS. All readers were blinded to patient demographics, treatment regimen, and tumor molecular subtypes. The term "overall agreement" was defined as when 3 or more examiners agreed and the term "overall disagreement" was defined as when 2 or more examiners disagreed. In cases with disagreement between reviewers, the cases were reanalyzed in a collaborative fashion by at least 3 examiners, and a consensus score was reached and used in the final analysis.

Based on the current available MR imaging literature and the cumulative experiences from the 2 tertiary centers, 7 imaging features were analyzed, as detailed in Table 1. These features included tumor margin: regular or irregular (Fig 1*A*, regular margin being a tumor with a smooth enhancing margin on postgadolinium T1 and irregular margin being a tumor that lacks a smooth enhancing margin on postgadolinium T1), fungating or nonfungating (Fig 1*B*, a fungating margin being a tumor with a thick heterogeneous "brush"-like enhancing rim and nonfungating margin being a tumor that lacks a thick heterogeneous "brush"-like enhancing rim), cystic component (Fig 1*C*), radiologic necrosis (Fig 1*D*), limited or extensive PTE (Fig 1*E*), multifocality (Fig 1*F*), and hemorrhage (Fig 1*G*).

The protocol for measuring PTE grade was based on that developed by Wu[5] and Hartmann.[22] The degree of the white matter edema was estimated on the basis of the maximal distance from the tumor margin to the furthest point of the white matter edema. The tumor's maximal dimension was estimated based on the maximal diameter of the tumor on any axis. When the degree of white matter edema was less or similar (no more than 4 mm greater) to the tumor's maximal dimension, the edema was considered low grade, and when the degree of white matter edema was greater (more than 4 mm) than the tumor's maximal dimension, the edema was considered a high-grade.

Furthermore, the Visually AcceSAble Rembrandt Images (VASARI) feature set was analyzed on 164 cases (https://wiki.cancerimagingarchive.net/display/Public/VASARI+Research+Project[18,23,24]); 16 cases were missing some sequences required for the VASARI analysis.

Telomere Maintenance Mechanism Subtyping

Tumors were classified into 4 subgroups: ALT positive tumors with or without a high content of tumor associated macrophages (ALT+/M+ and ALT+/M−, respectively) and ALT negative tumors with or without a high content of tumor associated macrophages (ALT−/M+ and ALT−/M−, respectively) based on established methods by using paraffin-embedded tumor sections.[4,25] Tumors from 80 cases were typed for

Table 1: Specific classification of MRI features

Imaging Feature with:	Classification Criteria
Regular enhancing margin	
Yes	Smooth enhancing margin on post-Gd T1
No	Lack of smooth enhancing margin on post-Gd T1
Fungating margin	
Yes	Thick heterogeneous brushlike enhancing rim on post Gd T1
No	Lack of thick heterogeneous brushlike enhacing rim on post-Gd T1
Cystic	
Yes	A well-circumscribed region with low T1 and high T2 signal; loses signal on the FLAIR sequence
No	Lack of well-circumscribed region with low T1 and high T2 signal; does not lose signal on the FLAIR sequence
Proportion of necrosis	
Yes	An area within the tumor that had high signal on T2 and low signal on T1; had heterogeneous enhancement on post-Gd T1; the proportion of the tumor estimated to represent more than 5% necrosis
No	Less than 5% or none
Proportion of edema[a]	
Limited (<50% of the entire abnormality)	Less than half of the entire abnormality is estimated to represent vasogenic edema
Extensive (> 50% of the entire abnormality)	More than half of the entire abnormality is estimated to represent vasogenic edema
Multifocal and multicentric lesion	
Yes	Two or more enhancing intra-axial tumors on post-Gd T1
No	One intra-axial tumor on post-Gd T1
Hemorrhage	
Yes	Tumor has an area of internal high or isolated T1 and low T2; area of internal high T1 and high T2; area of internal low T1 and low T2. Takes into account that the signal characteristics differ depending on the age of the hemorrhage. SWI sequences were also used.
No	No hemorrhage

Note:—Gd indicates gadolinium.

[a] The protocol for measuring PTE grade was based on that by Wu et al[5] and Hartmann et al.[22]

telomere maintenance mechanisms as part of an earlier study, and 100 tumors were new to this study.[4] The tumor-associated macrophage content was identified by immunohistochemistry staining for CD163 positive macrophages. The CD163 antibody used was EPR19518 (Abcam, Cambridge, United Kingdom), and the macrophage content was estimated as described previously.[4]

Mutant IDH1 *and* IDH2 *Determination*

The presence of the R132H IDH1 mutation was estimated by using immunohistochemistry.[26] To confirm the presence and frequency of *IDH1* mutations and to estimate the number of *IDH2* mutations, exon 4 of *IDH1* and *IDH2* were amplified from tumor-extracted DNA and sequenced.[27] Tumor DNA was extracted from paraffin embedded tumor sections or frozen tumor.

MGMT *Promoter Methylation Determination*

The method to determine whether tumors had a methylated or unmethylated *MGMT* promoter was based on published methods.[21,28] In this study, genomic DNA was extracted from paraffin-embedded tumors by using the QIAmp DNA FFPE tissue Kit (QIAGEN, Tokyo, Japan), and bisulfite DNA conversion was performed by using the EpiTect Bisulfite kit (QIAGEN).

Statistical Methods

The clinico-demographic and MR imaging features were compared between the 3 telomere maintenance–based subtypes by using Pearson χ^2 tests and 1-way ANOVA as appropriate. The κ statistical test was performed to assess the concordance between interobserver agreement. Logistic regression was used to test if imaging could predict the ALT+/M− and ALT−/M+ subtypes and used imaging features as covariants. Survival was compared between the subtypes by using the log-rank test and the independent association of the MR imaging features in addition to the subtype effects. To test multiple variants on survival, Cox proportional hazards regression models were used. A 2-tailed P value $<.05$ was taken to indicate statistical significance.

RESULTS

Whether the 7 internally derived MR imaging features could be consistently identified was investigated by comparing MR imaging scores from the 3 different readers and calculating the percentage of scans on which all 3 blinded reviewers agreed on the presence or absence of each MR imaging feature. κ statistical analyses were performed. The interobserver data including κ value demonstrated reproducible results (Table 2). The interobserver agreement rate was highest for the glioblastoma cystic component feature (86.2%, $\kappa = 0.71$), followed by multifocal lesion (85.6%, $\kappa = 0.71$). The margin-based parameters had the lowest interobserver agreement percentages (regular margin, 62.9%, $\kappa = 0.23$; fungating margin, 64.6%, $\kappa = 0.28$).

MR Imaging Features Predictive of ALT+ and M+ Status

In the 7 internally derived MR imaging feature groups, the clinico-demographic features and the frequency of *IDH1* and *IDH2* mutations and *MGMT* promoter methylation among the telomere maintenance subtypes are given in Table 3. Three telomere maintenance–based subtypes had sufficient numbers to investigate MR imaging features (ALT+/M−, $n = 26$; ALT−/M−, $n = 92$; and ALT−/M+, $n = 56$). Because of the lack of glioblastomas in the ALT+/M+ group ($n = 6$), these cases were not included in the subsequent analyses. The frequency of each MR imaging feature among the telomere-based subtypes is given in Table 4. Five MR imaging features—regular margin, fungating margin, tumor cystic component, radiologic necrosis, and limited

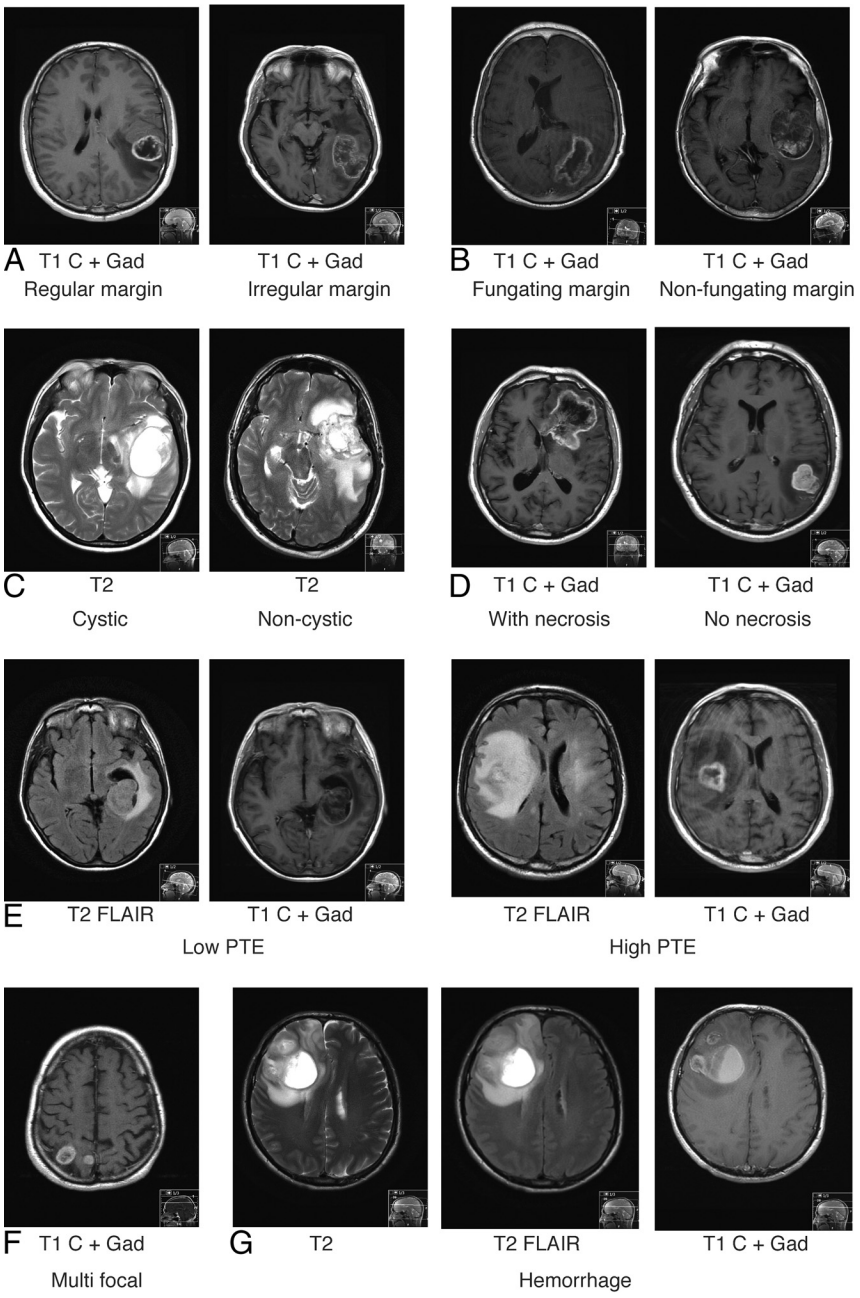

FIG 1. Examples of MR imaging features in glioblastoma. *A*, Tumor classified with a regular (*left*) or irregular margin (*right*). *B*, Tumor classified with a fungating (*left*) or nonfungating margin (*right*). *C*, Tumors classified with a cystic component (*left*) or noncystic component (*right*). *D*, Tumor classified with (*left*) and without (*right*) radiologic necrosis. *E*, Tumor classified with low (*limited, left*) and high (*extensive, right*) PTE. *F*, Tumor classified as being multifocal. *G*, tumor classified with hemorrhage. Gd indicated gadolinium; C, contrast.

Table 2: Interobserver reliability assessment for MRI features in glioblastoma

MRI Feature	% Where All 3 Reviewers Agree	κ Value
Regular margin	62.9%	0.23
Fungating margin	64.6%	0.28
Cystic	86.2%	0.71
Necrosis	72.6%	0.50
Limited PTE	70.7%	0.43
Hemorrhage	78.3%	0.56
Multifocal lesion	85.6%	0.71

or extensive PTE—showed altered frequency among the 3 tumor subgroups.

The ALT−/M+ subgroup had the lowest incidence of tumors with a cystic component (10.7%) compared with the ALT+/M− (38.5%) and the ALT−/M− (23.9%) groups ($P = .014$). This subtype had the highest incidence of tumors with extensive PTE (44.6% versus 23.1% for ALT+/M− and 22.8% for ALT−/M−, $P = .014$) and the highest incidence of tumors with radiologic necrosis (85.7% versus 72.8% for ALT−/M− and 58% for ALT+/M−; $P = .021$).

The ALT+/M− subgroup had the highest incidence of tumors with a regular margin (58% versus 30% in both the ALT−/M− and ALT−/M+ groups; $P = .026$) and the lowest incidence of tumors with a fungating margin (19% versus 53% and 61% in the ALT−/M− and ALT−/M+ groups, respectively; $P = .002$).

With the exception of PTE, the other MR imaging features were strongly associated with each other. Cystic tumors were more likely to have regular margins with no necrosis, and noncystic tumors were more likely to have irregular margins with necrosis (cystic association with regular margin, $P < .0001$; cystic with no necrosis, $P < .0001$).

To test whether imaging could predict ALT+/M− or an ALT−/M+ status, a logistic regression analysis was performed. For predicting ALT+/M− tumors, 3 features—cystic component (standard error, 1.18; $P = .0077$; OR, 0.04; 95% CI, 0.004–0.43), radiologic necrosis (standard error, 1.16; $P = .0001$; OR, 84; 95% CI, 8.6–821), and fungating margin (standard error, 0.61; $P = .015$; OR, 0.23; 95% CI, 0.07–0.75) showed statistical differences and were included in the final model. For predicting ALT−/M+ tumors, 2 features—extensive PTE (standard error, 0.48; $P = .007$; OR, 0.27; 95% CI, 0.11–0.7) and fungating margin (standard error, 0.36; $P = .014$; OR, 2.5; 95% CI, 1.2–4.8) showed statistical differences and were included in the final model.

Using the VARSARI feature set, 6 VASARI features—side of lesion center (F2), proportion of necrosis (F7), cysts (F8), T1/FLAIR ratio (F10), proportion of edema (F14), and ependymal extension (F19)—were found to be correlated with the 3 tumor subgroups. The full set of VASARI features and the associations with telomere maintenance glioblastoma subtypes is detailed in On-line Table 1.

Table 3: Clinico-demographic features among telomere maintenance glioblastoma subtypes

Demographics	Telomere Maintenance Subtype			Pearson χ^2 (or F-Ratio) and *P* Values[a]
	ALT+/M- (*n* = 26)	ALT-/M- (*n* = 92)	ALT-/M+ (*n* = 56)	
% Male (no.)	57.7 (15)	63 (58)	57.1 (32)	0.6, .742
Mean age (range), yrs	45.9 (16–66)	64.1 (40–81)	63.2 (39–82)	34.8, <.001
Median survival, mo	21.0	10.6	7.1	40.1, <.001
% Treated with at least 4 cycles of temozolomide (no.)	42.3 (11)	38 (35)	32 (18)	0.63, .629
% Treated with radiotherapy (no.)	84.6 (22)	78.3 (72)	92.9 (52)	5.5, .064
Type of surgery				
Biopsy, % (no.)	15.4 (4)	24 (22)	16 (9)	37.9, <.0001
Near total, % (no.)	76.9 (20)	61 (56)	27.3 (15)	
Partial	8 (2)	15.2 (14)	56.4 (31)	
MGMT promoter methylation status, % (no.)	61.5 (16)	45 (36)	48 (25)	NS
IDH1 and *IDH2* mutation status, % (no.)	73 (19)	9 (8)	5 (3)	67, <.0001

Note:—NS indicates not significant.
[a] Statistical comparisons were made between 3 groups: ALT+/M−, ALT−/M−, and ALT−/M+.

Table 4: MRI features among telomere maintenance glioblastoma subtypes

MRI Feature	Telomere Maintenance Subtype				
	ALT+/M-	ALT-/M-	ALT-/M+	Pearson χ^2 and *P* Values[a]	ALT+/M+
No. of patients	26	92	56		6
Regular margin, % (no.)	58 (15)	30 (28)	30 (17)	7.3, .026	33 (2)
Fungating margin, % (no.)	19 (5)	53 (49)	61 (34)	12.8, .002	67 (4)
Cystic component, % (no.)	39 (10)	24 (22)	11 (6)	8.5, .014	50 (3)
Radiologic necrosis, % (no.)	58 (15)	73 (67)	86 (48)	7.7, .021	83 (5)
Extensive PTE, % (no.)	23 (6)	23 (21)	45 (25)	8.6, .014	17 (1)
Multifocal lesion, % (no.)	15 (4)	12 (11)	23 (13)	NS	33 (2)
Hemorrhage, % (no.)	8 (2)	20 (18)	7 (4)	NS	3 (2)

Note:—NS indicates not significant.
[a] Statistical comparisons were made between 3 groups: ALT+/M−, ALT−/M−, and ALT−/M+.

Table 5: MRI features among mutant *IDH1* and *IDH2* tumors

MRI Feature	Tumor Type		
	IDH1 and *IDH2* Mutant (*n* = 30)	*IDH1* and *IDH2* Wild-Type (*n* = 150)	Pearson χ^2 and *P* Values
Regular margin	50%	31%	NS
Fungating margin	33%	55%	4.8 .028
Cystic component	37%	17%	5.7 .017
Radiologic necrosis	63%	77%	NS
Extensive PTE	23%	32%	NS
Multifocal lesion	10%	16%	NS
Hemorrhage	10%	15%	NS

Note:—NS indicates not significant.

The ALT−/M+ subgroup had the lowest incidence of tumors with a cyst (4%) compared with the ALT+/M− (30%) and the ALT−/M− (12%) groups ($P = .007$), the highest incidence of tumors with a higher proportion of necrosis (71%) versus 49% for ALT−/M− and 42% for ALT+/M ($P = .026$), and the highest incidence of tumors with the highest grade of edema (grade 5; 53%) compared with 32% in the ALT−/M− and 14% in the ALT+/M− group ($P = .002$).

The ALT+/M− subgroup had the highest incidence of tumors with an expansive T1/FLAIR ratio (79%) compared with 41% in the ALT−/M− and 37% in the ALT−/M+ group ($P = .0003$), the lowest incidence of tumors located in the right side of the brain (17%) compared with 41% in the ALT−/M− and 54% in the ALT−/M+ group ($P = .007$), and the lowest incidence of tumors with ependymal extension (30%) compared with 60% in the ALT−/M− and 49% in the ALT−/M+ group ($P = .036$).

To test whether the VASARI imaging features could predict ALT+/M− or an ALT−/M+ status, a logistic regression analysis was performed. For predicting ALT+/M− tumors, 3 features were significant—F2 side of lesion center % left (standard error, 0.52; $P = .049$; OR, 2.8; 95% CI, 1.01–7.8), F8 cysts (standard error, 0.57; $P = .04$; OR, 3.2, 95% CI, 1.05–9.8), and F10 T1/FLAIR ratio % expansive (standard error, 0.52; $P = .016$; OR, 3.5; 95% CI, 1.26–9.7). To predict ALT−/M+ status, only 1 feature was significant: F8 cysts (standard error, 0.77; $P = .03$; OR, 0.19; 95% CI, 0.04–0.87).

MR Imaging Features Correlated with IDH1 *and* IDH2 *Mutations*

In the 7 internally derived MR imaging feature groups, the mutant *IDH1* or mutant *IDH2* was present in 30 tumors; this included most ALT+/M− ($n = 19/26$, 73%; Table 3) tumors and was less frequent in ALT−/M− ($n = 8/92$, 9%) and ALT−/M+ tumors ($n = 3/56$, 5%).

Tumors with mutant *IDH1* and *IDH2* had a higher incidence of the cystic component feature (37%) compared with tumors with wild-type *IDH1* and *IDH2* (17%, $P = .017$) and fewer incidences of tumors with a fungating margin (33%) compared with wild-type tumors (55%, $P = .028$; Table 5). Using the VASARI features, patients with mutant *IDH1* and *IDH2* glioblastomas had a higher incidence of tumors with an expansive T1/FLAIR ratio (80%) compared with the wild-type tumors (40%, $P < .0001$) and a lower incidence of grade 5 edema (17%) compared with wild-type tumors (38%, $P = .024$; On-line Table 2).

MR Imaging Features Predict Survival Beyond Molecular Status

Consistent with earlier studies, the ALT+/M− subgroup patients had the best survival (Fig 2), and the ALT−/M− subgroup patients had an improved overall survival compared with the

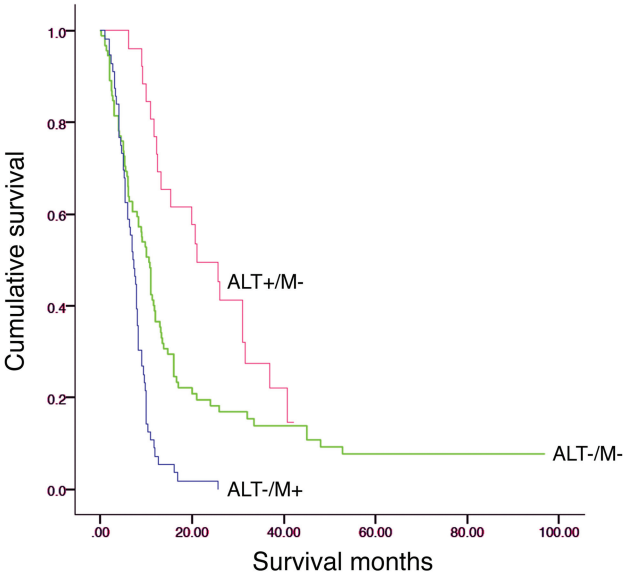

FIG 2. The 3 telomere maintenance mechanism subtypes are associated with differences in patient survival. Eighty cases were those used in a previous study,[4] and 100 cases were new to this study.

Table 6: Cox regression analysis to test if radiology features added to telomere maintenance subtype and *MGMT* promoter methylation status in predicting patient survival

Category Variable	Wald Value	*df*	Significance *P*
Molecular subtype	26	2	<.0001
MGMT	6.89	1	.009
Cystic	4	1	.045

ALT−/M+ group (Fig 2, $P < .009$ ALT+/M− versus ALT−/M−, $P < .0001$ ALT+/M− versus ALT−/M+, and ALT−/M− versus ALT−/M+ $P < .001$).[3,4,29] There were no significant differences ($P > .05$) among telomere maintenance–based subgroups in relation to the amount of patients treated with radiation therapy, concurrent temozolomide, or adjuvant temozolomide. In an earlier study and in this study (Table 4), the ALT−/M+ subgroup was associated with an increased frequency of partial resections compared with near-total resections.[4]

A Cox regression analysis by using forward and backward stepwise models was used to determine whether 4 imaging features (margin regularity, cystic, necrosis, and PTE grade) added to telomere maintenance–based subtype and *MGMT* promoter methylation status to better determine patient prognosis. Cystic feature was significant ($P = .045$) in predicting patients' survival independent of tumor subtype and *MGMT* promoter methylation status (Table 6).

DISCUSSION

An assessment of MR imaging features is an advantage to using histologic-based subtypes alone because the characteristics of whole tumor in situ can be assessed before surgery. In this study, we found radiologic features (including the VASARI MR imaging) associated with telomere maintenance and tumor-associated macrophage content–based subtypes, consistent with MR imaging features being informative in identifying differences in tumor biology. A cystic component was additive in predicting an improved patient outcome, suggesting that inclusion of this MR imaging feature along with an assessment of telomere maintenance subtypes and *MGMT* promoter methylation status will improve patient outcome prediction. Both feature sets had imaging parameters that predicted the ALT+/M− and the ALT−/M+ subgroups.

Because temozolomide use ALT−/M+ tumors are associated with the poorest survival independent of patient age, extent of surgery, and treatment received.[4] ALT−/M+ tumors were associated with a higher proportion of necrosis, extensive edema, and lack of a cystic component. Whether the increased macrophage content directly contributes to the associated MR imaging features is unknown. Tumor-associated macrophages have many tumor-promoting activities including proinvasive and proangiogenesis properties.[30] Increased edema may result from increased vascular permeability. Increased vascular endothelial growth factor and angiogenesis correlated with edema,[31,32] and a molecular marker found on endothelial cells (deltalike ligand 4) that functions in angiogenesis was associated with PTE and poorer patient survival.[33] Consistent with a link between PTE and angiogenesis, patients treated with the vascular endothelial growth factor inhibitor bevacizumab had reduced PTE.[34]

Increased edema has been associated with poorer prognosis.[6-8] In the study by Carillo et al,[13] edema was additive for survival for *MGMT* methylated but not unmethylated tumors. In the current study, edema was not additive to survival by tumor subtype; this is likely attributable to edema being closely associated with the ALT−/M+ subtype. In a future study, we aim to incorporate quantitative MR imaging techniques, more specifically DTI in vivo to demonstrate the PTE grade.[35] The imaging features associated with the ALT−/M+ group are consistent with this subgroup comprising aggressive tumors. The increased content of macrophages in the ALT−/M+ subtype, combined with these tumors having a poorer prognosis that has not changed with temozolomide, suggests this subtype would be an ideal target for immunotherapies, particularly those that could activate macrophages to remove the malignant cells or those that inhibit the tumor-promoting activities of tumor-associated macrophages.[4,36]

Alternative lengthening of telomere-positive tumors is associated with the best overall patient survival independent of patient age, extent of surgery, treatment received, and *IDH1* mutant status.[3,4,29] In this study, ALT+ tumors were more likely to have a regular margin, lack of a fungating margin, cystic component, expansive T1/FLAIR ratio, and lack of ependymal extension, consistent with ALT+ tumors being less aggressive. The MR imaging data from other studies support ALT+ tumors being less aggressive.[29,37,38] Sharper margins and less contrast enhancement by MR imaging have been associated with features of ALT+ tumors, including mutant *IDH1*, mutant tumor protein p53 (*TP53*), or proneural tumors.[13,16,18,20,39,40] Considering that most ALT+tumors in this study had mutant *IDH1* or *IDH2*, MR imaging features of ALT may be due to mutant *IDH*. The expansive T1/FLAIR VASARI feature had greater significance when tumors were compared based on *IDH* mutant status rather than telomere maintenance subtype.

The presence of the cystic component was associated with improved survival. A cystic component has been associated with improved survival in some,[9,10] but not all studies.[6,12,13] If molec-

ular differences are driving phenotypes that are detected by MR imaging, inconsistencies between studies may be improved if the molecular subgroups are included in analyses of MR imaging features. Tumors that were ALT+/M− and ALT−/M− had a higher cystic component compared with non-ALT+/M+ tumors. In a study by Carrillo et al,[13] a cystic component was one of 4 features that could predict mutant *IDH1* glioma with 94% accuracy. A cystic component associated with mutant *IDH1* could explain the higher incidence of the cystic component in ALT+ tumors. Similarities exist between clinical parameters for those with cystic glioblastoma and those with secondary glioblastoma, suggesting the cystic component may indicate those with previously undiagnosed low-grade glioma. This may be the case for those with ALT+ tumors because ALT+/M− is more frequent in secondary glioblastoma. A cystic component was present in a considerable portion of ALT−/M− tumors; fewer of these had mutant *IDH1* ($n = 3/22$, 13%), and most are thought to arise de novo.

The cystic component in ALT−/M− tumors may arise because of a different mechanism to that in ALT+ tumors. Why ALT−/M− tumors with a cystic component are associated with improved survival is unclear. The cystic component may represent a distinct tumor biology that responds well to treatment, or it may directly aid in the acquisition or detainment of temozolomide. The cystic component was reproducibly identified among different radiologists. A larger study to investigate whether ALT−/M− tumors with a cystic component are those that respond well to temozolomide is warranted.

Limitations of this study include its retrospective nature. The study excluded patients previously treated with radiation therapy to prevent factors that would affect MR imaging interpretation. This would exclude more patients with secondary glioblastoma that are more likely to be ALT+. Thus, the MR imaging features of the ALT+ group will be representative of a subset of ALT+ tumors.

CONCLUSIONS

The radiologic feature of cystic component was a predictive factor for survival and could be combined with telomere maintenance mechanism and macrophage content–based subtypes and *MGMT* promoter methylation status to provide a better estimation of survival. A lack of cystic component, a lack of left-sided tumor epicenter, higher necrosis and edema, along with a higher ependymal extension are more often present in tumors with a high tumor-associated macrophage content, suggesting that the presence of macrophages leads to a more invasive tumor behavior and a greater difficulty in obtaining near total resection, which could be predicted by MR imaging.

ACKNOWLEDGMENTS

We would like to acknowledge Dr James Fulton for his MR imaging expertise, Mrs Amanda Fisher, Ms Sara Bowie, and Ms Janine Neill for their technical assistance, Ms Helen Morrin and the Cancer Society Tissue Bank, and Mr David Wong for his contribution to data collection.

Disclosures: Jean Zhou—*RELATED*: *Grant*: Health Research Council of New Zealand, *Comments*: titled "Molecular subtypes of glioblastoma predicts tumour behavior"*; *UNRELATED*: *Employment*: Southern District Health Board, *Comments*: Radiology registrar in Dunedin Hospital, Otago, New Zealand; *Grants/Grants Pending*: Health Research Council, *Comments*: grant will be used to work on glioblastoma subtyping and imaging clinical trial with ultrasmall superparamagnetic iron oxide particles*. Michael V. Reddy—*UNRELATED*: *Board Membership*: Pacific Radiology Group, *Comments*: a private diagnostic radiology practice; *Employment*: Pacific Radiology Group and Southern District health Board, *Comments*: public and private radiology groups for whom I provide radiology services. Ramona A. Eiholzer—*RELATED*: *Grant*: Health Research Council of New Zealand*. Tania Slatter—*RELATED*: *Grant*: Health Research Council New Zealand*. *Money paid to the institution.

REFERENCES

1. Stupp R, Mason WP, van den Bent MJ, et al. **Radiotherapy plus concomitant and adjuvant temozolomide for glioblastoma.** *N Engl J Med* 2005;352:987–96 CrossRef Medline
2. Pickett HA, Reddel RR. **Molecular mechanisms of activity and derepression of alternative lengthening of telomeres.** *Nat Struct Mol Biol* 2015;22:875–80 CrossRef Medline
3. Hakin-Smith V, Jellinek DA, Levy D, et al. **Alternative lengthening of telomeres and survival in patients with glioblastoma multiforme.** *Lancet* 2003;361:836–38 CrossRef Medline
4. Hung NA, Eiholzer RA, Kirs S, et al. **Telomere profiles and tumor-associated macrophages with different immune signatures affect prognosis in glioblastoma.** *Mod Pathol* 2016;29:212–26 CrossRef Medline
5. Wu CX, Lin GS, Lin ZX, et al. **Peritumoral edema on magnetic resonance imaging predicts a poor clinical outcome in malignant glioma.** *Oncol Lett* 2015;10:2769–76 CrossRef Medline
6. Pope WB, Sayre J, Perlina A, et al. **MR imaging correlates of survival in patients with high-grade gliomas.** *AJNR Am J Neuroradiol* 2005;26:2466–74 Medline
7. Li WB, Tang K, Chen Q, et al. **MRI manifestions correlate with survival of glioblastoma multiforme patients.** *Cancer Biol Med* 2012;9:120–23 CrossRef Medline
8. Schoenegger K, Oberndorfer S, Wuschitz B, et al. **Peritumoral edema on MRI at initial diagnosis: an independent prognostic factor for glioblastoma?** *Eur J Neurol* 2009;16:874–78 CrossRef Medline
9. Maldaun MV, Suki D, Lang FF, et al. **Cystic glioblastoma multiforme: survival outcomes in 22 cases.** *J Neurosurg* 2004;100:61–67 CrossRef Medline
10. Utsuki S, Oka H, Suzuki S, et al. **Pathological and clinical features of cystic and noncystic glioblastomas.** *Brain Tumor Pathol* 2006;23:29–34 CrossRef Medline
11. Hammoud MA, Sawaya R, Shi W, et al. **Prognostic significance of preoperative MRI scans in glioblastoma multiforme.** *J Neurooncol* 1996;27:65–73 CrossRef Medline
12. Kaur G, Bloch O, Jian BJ, et al. **A critical evaluation of cystic features in primary glioblastoma as a prognostic factor for survival.** *J Neurosurg* 2011;115:754–59 CrossRef Medline
13. Carrillo JA, Lai A, Nghiemphu PL, et al. **Relationship between tumor enhancement, edema, IDH1 mutational status, MGMT promoter methylation, and survival in glioblastoma.** *AJNR Am J Neuroradiol* 2012;33:1349–55 CrossRef Medline
14. Pierallini A, Bonamini M, Osti MF, et al. **Supratentorial glioblastoma: neuroradiological findings and survival after surgery and radiotherapy.** *Neuroradiology* 1996;38 Suppl 1:S26–30 CrossRef Medline
15. Drabycz S, Roldán G, de Robles P, et al. **An analysis of image texture, tumor location, and MGMT promoter methylation in glioblastoma using magnetic resonance imaging.** *Neuroimage* 2010;49:1398–405 CrossRef Medline
16. Qi S, Yu L, Li H, et al. **Isocitrate dehydrogenase mutation is associated with tumor location and magnetic resonance imaging characteristics in astrocytic neoplasms.** *Oncol Lett* 2014;7:1895–902 CrossRef Medline
17. Liu XY, Gerges N, Korshunov A, et al. **Frequent ATRX mutations and loss of expression in adult diffuse astrocytic tumors carrying IDH1/IDH2 and TP53 mutations.** *Acta Neuropathol* 2012;124:615–25 CrossRef Medline
18. Gutman DA, Dunn WD Jr, Grossmann P, et al. **Somatic mutations**

associated with MRI-derived volumetric features in glioblastoma. *Neuroradiology* 2015;57:1227–37 CrossRef Medline
19. Aghi M, Gaviani P, Henson JW, et al. **Magnetic resonance imaging characteristics predict epidermal growth factor receptor amplification status in glioblastoma.** *Clin Cancer Res* 2005;11:8600–05 CrossRef Medline
20. Gutman DA, Cooper LA, Hwang SN, et al. **MR imaging predictors of molecular profile and survival: multi-institutional study of the TCGA glioblastoma data set.** *Radiology* 2013;267:560–69 CrossRef Medline
21. Hegi ME, Diserens AC, Gorlia T, et al. **MGMT gene silencing and benefit from temozolomide in glioblastoma.** *N Engl J Med* 2005;352:997–1003 CrossRef Medline
22. Hartmann M, Jansen O, Egelhof T, et al. **Effect of brain edema on the recurrence pattern of malignant gliomas** [Article in German]. *Radiologe* 1998;38:948–53 CrossRef Medline
23. Rios Velazquez E, Meier R, Dunn WD, Jr., et al. **Fully automatic GBM segmentation in the TCGA-GBM dataset: prognosis and correlation with VASARI features.** *Sci Rep* 2015;5:16822 CrossRef Medline
24. Gevaert O, Mitchell LA, Achrol AS, et al. **Glioblastoma multiforme: exploratory radiogenomic analysis by using quantitative image features.** *Radiology* 2014;273:168–74 CrossRef Medline
25. Henson JD, Hannay JA, McCarthy SW, et al. **A robust assay for alternative lengthening of telomeres in tumors shows the significance of alternative lengthening of telomeres in sarcomas and astrocytomas.** *Clin Cancer Res* 2005;11:217–25 Medline
26. Capper D, Weissert S, Balss J, et al. **Characterization of R132H mutation-specific IDH1 antibody binding in brain tumors.** *Brain Pathol* 2010;20:245–54 CrossRef Medline
27. Royds JA, Pilbrow AP, Ahn A, et al. **The rs11515 polymorphism is more frequent and associated with aggressive breast tumors with increased ANRIL and decreased p16 (INK4a) expression.** *Front Oncol* 2015;5:306 CrossRef Medline
28. Palmisano WA, Divine KK, Saccomanno G, et al. **Predicting lung cancer by detecting aberrant promoter methylation in sputum.** *Cancer Res* 2000;60:5954–58 Medline
29. McDonald KL, McDonnell J, Muntoni A, et al. **Presence of alternative lengthening of telomeres mechanism in patients with glioblastoma identifies a less aggressive tumor type with longer survival.** *J Neuropathol Exp Neurol* 2010;69:729–36 CrossRef Medline
30. Ludwig HC, Feiz-Erfan I, Bockermann V, et al. **Expression of nitric oxide synthase isozymes (NOS I-III) by immunohistochemistry and DNA in situ hybridization. Correlation with macrophage presence, vascular endothelial growth factor (VEGF) and oedema volumetric data in 220 glioblastomas.** *Anticancer Res* 2000;20:299–304 Medline
31. Senger DR, Galli SJ, Dvorak AM, et al. **Tumor cells secrete a vascular permeability factor that promotes accumulation of ascites fluid.** *Science* 1983;219:983–85 CrossRef Medline
32. Carlson MR, Pope WB, Horvath S, et al. **Relationship between survival and edema in malignant gliomas: role of vascular endothelial growth factor and neuronal pentraxin 2.** *Clin Cancer Res* 2007;13:2592–98 CrossRef Medline
33. Qiu XX, Wang CH, Lin ZX, et al. **Correlation of high delta-like ligand 4 expression with peritumoral brain edema and its prediction of poor prognosis in patients with primary high-grade gliomas.** *J Neurosurg* 2015;123:1578–85 CrossRef Medline
34. Jain RK, Tong RT, Munn LL. **Effect of vascular normalization by antiangiogenic therapy on interstitial hypertension, peritumor edema, and lymphatic metastasis: insights from a mathematical model.** *Cancer Res* 2007;67:2729–35 CrossRef Medline
35. Pierpaoli C, Jezzard P, Basser PJ, et al. **Diffusion tensor MR imaging of the human brain.** *Radiology* 1996;201:637–48 CrossRef Medline
36. Mantovani A, Marchesi F, Malesci A, et al. **Tumour-associated macrophages as treatment targets in oncology.** *Nat Rev Clin Oncol* 2017;14:399–416 CrossRef Medline
37. Royds JA, Al Nadaf S, Wiles AK, et al. **The CDKN2A G500 allele is more frequent in GBM patients with no defined telomere maintenance mechanism tumors and is associated with poorer survival.** *PloS One* 2011;6:e26737 CrossRef Medline
38. Chen YJ, Hakin-Smith V, Teo M, et al. **Association of mutant TP53 with alternative lengthening of telomeres and favorable prognosis in glioma.** *Cancer Res* 2006;66:6473–76 CrossRef Medline
39. Metellus P, Coulibaly B, Colin C, et al. **Absence of IDH mutation identifies a novel radiologic and molecular subtype of WHO grade II gliomas with dismal prognosis.** *Acta Neuropathol* 2010;120:719–29 CrossRef Medline
40. Wang YY, Wang K, Li SW, et al. **Patterns of tumor contrast enhancement predict the prognosis of anaplastic gliomas with IDH1 mutation.** *AJNR Am J Neuroradiol* 2015;36:2023–29 CrossRef Medline